

Self-calibration of a moving zoom-lens camera by pre-calibration¹

Peter Sturm*

GRAVIR-IMAG and INRIA Rhône-Alpes, 655, Avenue de l'Europe, 38330 Montbonnot, France

Abstract

We consider the problem of self-calibrating a moving camera which is equipped with a zoom lens. This consists essentially in estimating the 5 intrinsic parameters of the pinhole camera model. However, these parameters are not independent, subject to zooming. Thus, we propose to do a pre-calibration of the camera, with the aim to model the interdependence of the intrinsic parameters. We show that self-calibration then comes down to the estimation of only one intrinsic parameter. We propose a method which exploits this and which does not need an initialization of the intrinsic parameters. © 1997 Elsevier Science B.V.

Keywords: Self-calibration; Zoom; Pre-calibration

1. Introduction

In this paper we address the problem of self-calibration of a moving camera. This means essentially the determination of the camera's intrinsic parameters, only from the information of image feature correspondences. In the pioneering work of Maybank and Faugeras [1], the authors consider constraints on the intrinsic parameters which arise from the rigidity of the camera motion and which are based on the epipolar geometry of two views. These constraints are known as Kruppa's equations. Experimentations with methods based on these equations reveal imprecision and inaccuracy due to high sensitivity to noise, and also convergence problems [2].

To moderate these effects, it is proposed to reduce the number of unknowns by fixing some of the intrinsic parameters to predefined values [2–4]. While there is no problem for fixing the aspect ratio and the skew of the pixel coordinate axes, which are very stable over long time periods, the position of the principal point depends on the zooming position and lens focus of the camera [5,6] (see Fig. 1). This phenomenon is due to optical and mechanical misalignments in the lens system of a camera and can occur in such an extreme manner as shown in Fig. 5, where the

coordinates of the principal point vary up to 100 pixels while zooming!

On one hand, this illustrates that fixing the position of the principal point can bias heavily the results of self-calibration. On the other hand, although the intrinsic parameters are correlated, the correlation seems to be simple and stable.

This led to the idea that, if it is possible to obtain a simple analytical model which approximates the behaviour of intrinsic parameters as a function of other parameters, this knowledge could be introduced into any self-calibration method in order to reduce the number of unknowns and to improve the accuracy of the results. Thus, we want to model the *interdependence* of intrinsic parameters, concretely between the position of the principal point and the horizontal and vertical scale factors.

We propose to precede the application of a dynamic vision system by a pre-calibration stage, where a model for the interdependence of intrinsic parameters is established. We show, that dynamic self-calibration may then be reduced to the estimation of one parameter, on which the other parameters depend. The advantages of this approach are a simpler and faster computation, higher accuracy and no need of an initial estimation, thanks to the off-line elimination of correlation.

The paper is organized as follows. We first discuss the pinhole camera model and especially several aspects of the intrinsic parameters. Next, Kruppa's equations are derived and it is shown how to use them for self-calibration.

* Tel.: +33 4 7661 5232; fax: +33 4 7661 5210; e-mail: Peter.Sturm@inrialpes.fr.

¹ This work has been done in the context of the MOVI project which belongs to CNRS, INPG, INRIA and UJF.

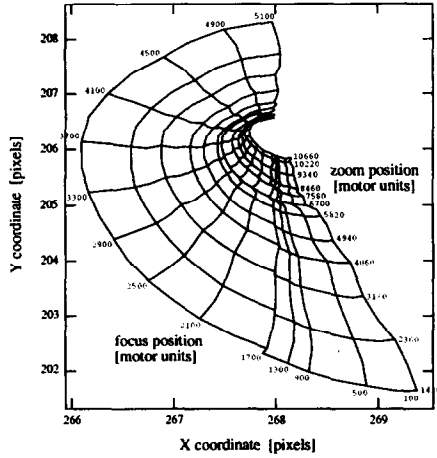


Fig. 1. Image center as a function of lens focus and zoom motors [5].

We then show how information on the interdependence of intrinsic parameters can be introduced in the self-calibration process. Based on this consideration, we propose a self-calibration method, which exploits this information. Then results of experiments with the self-calibration method are reported. Finally, we discuss our observations and propositions and indicate how this work can be extended.

2. Intrinsic parameters of a zooming camera

2.1. The pinhole model

In the following we model cameras by the pinhole scheme which is a good approximation to the physical reality. A camera is represented by a *projection center* O and a *retinal plane* \mathcal{R} . The projection q of a 3D point Q is the intersection of the line $\langle O, Q \rangle$, with the retinal plane. This projection can be represented by a 3×4 projection matrix P such that $q \sim PQ$, where Q and q are represented by homogeneous coordinates and \sim means equality up to a scalar factor. The *optical axis* is the line through the projection center and perpendicular to the retinal plane. Its intersection with the retinal plane is the *principal point*.

2.2. Extrinsic and intrinsic parameters

We can identify two groups of physically meaningful parameters which describe entirely the pinhole projection: 6 extrinsic parameters stand for the position and orientation of the camera, and 5 intrinsic parameters characterize the camera's projection properties. The intrinsic parameters are:

- u_0 and v_0 , the coordinates of the principal point;
- α_u and α_v , the horizontal and vertical scale factors;
- θ , the skew angle between the coordinate axes in the pixel coordinate system.

The projection matrix can be decomposed as

$$P = A \left(\begin{array}{c|c} R & -Rt \end{array} \right) = \begin{pmatrix} \alpha_u & -\alpha_u \cot \theta & u_0 \\ 0 & \alpha_v / \sin \theta & v_0 \\ 0 & 0 & 1 \end{pmatrix} \left(\begin{array}{c|c} R & -Rt \end{array} \right)$$

where A is the *calibration matrix* of the camera, t the position of the projection center and the orthonormal matrix R represents the camera's orientation.

2.3. The absolute conic and the intrinsic parameters

Let Ω be the absolute conic, i.e. the conic which is formed by the points $(x, y, z, w)^T \in \mathcal{P}^3$ with $x^2 + y^2 + z^2 = 0$ and $w = 0$ (see [7]). An interesting property of this conic is that its projection ω depends only on the intrinsic parameters of a camera, i.e. ω is fixed for a moving camera with fixed intrinsic parameters. The projection of the absolute conic by a camera with calibration matrix A is given by [2]

$$C^* \sim AA^T$$

where C is the matrix representation of ω and C^* denotes its dual matrix.² Determination of the intrinsic parameters is equivalent to determination of the projection of the absolute conic, since A may be uniquely computed from C by Cholesky decomposition. This principle is used for self-calibration via Kruppa's equations (see Section 3.2).

2.4. Stability of the intrinsic parameters

Some of the intrinsic parameters are constant over long time periods. Especially, the *aspect ratio* $\tau = \alpha_u / \alpha_v$ and the skew angle θ do not change in general. In practice θ is often very close to 90° . So, in many works concerning calibration or self-calibration, θ is assumed to be 90° and is not estimated.

As for the principal point, it has been shown that it is not stable, rather its position varies when the zoom position and the lens focus change [5,6]. These authors have observed that zooming causes the principal point to move on a nearly translational trajectory (for most zoom objectives). However, in the following we will not restrict ourselves to the case of a translation, rather we consider a generic model. The reasons for this phenomenon are optical and mechanical misalignments in the lens system of a camera.

In the following we suppose that the influence on the intrinsic parameters comes mainly from the zoom position and neglect the effects of changing the focus. The focus

² The dual to a conic C of points is the conic which consists of the tangent lines of C .

however, will affect the pre-calibration proposed in Section 4. In the concluding Section 7, we propose a mechanism for dealing with this problem.

2.5. Interdependence of intrinsic parameters

Despite the revelation of the influence of zooming on the parameters α_u , α_v , u_0 and v_0 , the interdependence of these parameters, subject to zooming, has to our knowledge not yet been used in the context of self-calibration. We want to profit from these interdependencies and try therefore to obtain an analytical model which expresses the intrinsic parameters as functions of one of them, say α_v , (the skew angle θ is considered to be fixed):

$$A = \begin{pmatrix} \alpha_u(\alpha_v) & -\alpha_u(\alpha_v)\cot\theta & u_0(\alpha_v) \\ 0 & \alpha_v/\sin\theta & v_0(\alpha_v) \\ 0 & 0 & 1 \end{pmatrix}.$$

For the horizontal scale factor we always have the relation

$$\alpha_u(\alpha_v) = \tau \frac{\alpha_v}{\sin\theta},$$

whereas the functional relationships $u_0(\alpha_v)$ and $v_0(\alpha_v)$ are more difficult to model.

In the following we call *pre-calibration* of a camera the off-line determination of the aspect ratio τ , the functional relationships $u_0(\alpha_v)$ and $v_0(\alpha_v)$, and the skew angle θ . If a camera is pre-calibrated, self-calibration will therefore be reduced to the estimation of the sole parameter α_v , and it will be possible to develop special methods exploiting this. We will discuss this in Sections 4 and 5.

3. Self-calibration of a moving camera

3.1. Problem specification

By self-calibration we mean the estimation of the intrinsic parameters of a camera, by just pointing it at a rigid scene. Especially, no 3D model of the scene and no information on the camera motion are available. The only information needed are correspondences of image points (or other features).

In this paper, we adopt the self-calibration approach which is based on Kruppa's equations, however the remarks on self-calibration of a pre-calibrated camera in Section 5 are also valid for other paradigms [8,9].

In the sequel, we suppose the epipolar geometry of pairs of views known (it can be computed from point matches). We use its representation by the *fundamental matrix* F [10] which includes the position of the epipoles e and e' .

3.2. Kruppa's equations

The classical (though recent) self-calibration approach in

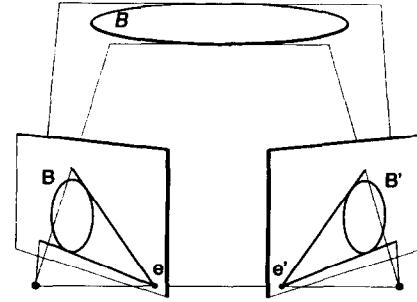


Fig. 2. Illustration of the epipolar matching constraint for conics. Tangent planes on 3D conics containing the baseline are projected onto corresponding epipolar lines tangent to the image conics.

the computer vision domain is based on *Kruppa's equations* [1]. If we assume that the intrinsic parameters are the same for two positions of one camera, then constraints on the projection of the absolute conic can be derived from the epipolar geometry of the two positions. This will be described in the following.

Let B and B' be the corresponding projections of a 3D conic \mathcal{B} in two views (see Fig. 2). There are two planes which contain the baseline of the views (the line joining the projection centers) and which are tangent to \mathcal{B} . Since these planes contain both projection centers, they are projected on corresponding epipolar lines which are tangent to B respectively B' . We derive a kind of "epipolar constraint" for the matching of projections B and B' of a 3D conic: if B and B' are in correspondence, then the epipolar line corresponding to an epipolar line tangent to B is tangent to B' , and vice versa. This can be written as³

$$(e \wedge q)^T B^* (e \wedge q) = 0 \Leftrightarrow (Fq)^T (B')^* (Fq) = 0. \quad (1)$$

Tangent planes on 3D conics containing the baseline are projected on corresponding epipolar lines tangent to the image conics.

Considering eqn (1) for the absolute conic and since its projection by a camera with invariant intrinsic parameters is fixed, we get

$$(e \wedge q)^T K (e \wedge q) = 0 \Leftrightarrow (Fq)^T K (Fq) = 0, \quad (2)$$

where $K = C^*$ is the matrix representation of the dual conic to ω . If we suppose that the epipole e is not at infinity, we can parameterize the first epipolar pencil by the points $(1, t, 0)^T$ and eqn (2) becomes

$$\begin{aligned} (e \wedge (1, t, 0)^T)^T K (e \wedge (1, t, 0)^T) &= 0 \\ \Leftrightarrow (F(1, t, 0)^T)^T K (F(1, t, 0)^T) &= 0. \end{aligned}$$

The two terms of this equivalence are quadratic polynomials in t . Thus, we can formulate the equivalence as

$$c_2 t^2 + c_1 t + c_0 = 0 \Leftrightarrow c_2' t^2 + c_1' t + c_0' = 0$$

where the coefficients c_i and c_i' depend on F , e and K . This condition leads finally to the three Kruppa equations of a

³ \wedge denotes the cross-product.

pair of views:

$$c_2 c_1' = c_1 c_2', \quad c_2 c_0' = c_0 c_2', \quad c_1 c_0' = c_0 c_1'. \quad (3)$$

Only two of them are algebraically independent.

3.3. Kruppa's equations and self-calibration

When the epipolar geometry, i.e. F and e , is known, the eqn (3) are constraints on K and hence on the intrinsic parameters. Thus they can be used for self-calibration. The usual approach of self-calibration consists in minimizing the criterion [2]

$$\sum_{p=1}^{\text{pairs of views}} \left(\frac{c_{p2}}{c'_{p2}} - \frac{c_{p1}}{c'_{p1}} \right)^2 + \left(\frac{c_{p2}}{c'_{p2}} - \frac{c_{p0}}{c'_{p0}} \right)^2 + \left(\frac{c_{p1}}{c'_{p1}} - \frac{c_{p0}}{c'_{p0}} \right)^2. \quad (4)$$

It is known that this estimation process is very sensitive to noise. Thus, several researchers tried to reduce the number of unknowns by fixing some of the intrinsic parameters. In [3], the skew angle and the coordinates of the principal point are fixed and the aspect ratio is supposed to be known. So, there remains only one parameter to estimate.⁴

However, especially fixing the principal point is not always corresponding to the physical reality of a zoom lens, as we stated in Section 2.4. We therefore generalize this approach in the next section, using generic models of the interdependence of intrinsic parameters.

4. Pre-calibration

In this section, we discuss how the interdependence of the intrinsic parameters can be modelled and how this affects Kruppa's equations.

4.1. Modelling the interdependence of intrinsic parameters

We suppose that the relation between the horizontal and vertical scale factors is given by $\alpha_u = \tau \alpha_v$, with the constant aspect ratio τ . Furthermore, the skew angle θ is constant (90°) and hence does not depend on other parameters. As for the coordinates of the principal point, we try to model them by functional relationships on α_v . Here we restrict ourselves to polynomial models, i.e.

$$u_0(\alpha_v) = c_m \alpha_v^m + \dots + c_1 \alpha_v + c_0, \quad (5)$$

$$v_0(\alpha_v) = d_n \alpha_v^n + \dots + d_1 \alpha_v + d_0.$$

To determine the degrees m and n and the coefficients c_i and d_i of the models, the camera has to be calibrated by a classical method [11] for several zoom positions, which results in an array of parameter values (see Fig. 5). From these, c_i and d_i can be obtained such that the model approximates well the calibration data. To obtain a sufficiently good model, but of minimal degree m respectively n , a robust regression method [12] can be applied.

4.2. How do interdependencies affect Kruppa's equations?

The Kruppa eqn (3) have the following form (the coefficients of the terms are not presented; these depend on the epipolar geometry):⁵

$$\begin{aligned} 0 = & \alpha_v^4 \\ & + \alpha_v^2 (u_0^2 + v_0^2 + u_0 v_0 + u_0 + v_0 + 1) \\ & + \alpha_v^0 (u_0^4 + u_0^3 v_0 + u_0^2 v_0^2 + u_0 v_0^3 + v_0^4 + u_0^3 + u_0^2 v_0 + u_0 v_0^2 \\ & + v_0^3 + u_0^2 + \dots + 1). \end{aligned}$$

Thus, if u_0 and v_0 are modelled as in eqn (5), Kruppa's equations become polynomials in the sole parameter α_v , of degree $\max\{4, 4\max\{m, n\}\}$.

In the following, we discuss first the special cases $m = n = 0$ and $m = n = 1$ and then the general case.

$m = n = 0$: *fixed principal point*. This case has already been considered in [3]. It is interesting to note that here, Kruppa's equations have the form

$$a \alpha_v^4 + b \alpha_v^2 + c = 0.$$

Hence, we obtain α_v by solving quadratic polynomials which leads to a closed-form solution of the problem.

$m, n \leq 1$: *translating principal point*. Kruppa's equations are general polynomials of degree 4, i.e. also the odd coefficients may be non-zero. Hence, there exists also a closed-form solution for finding possible candidates for α_v .

$m > 1$ or $n > 1$. Kruppa's equations are of degree greater than 5. There is no analytical solution, however, since the equations are univariate polynomials, their roots can be easily computed by numerical techniques.

5. A method of self-calibration based on pre-calibration of the camera

In this section, we are interested in how self-calibration methods can be simplified and made more accurate, when an analytical expression of the interdependence of intrinsic

⁴ To be precise, in [3] two cameras with possibly different intrinsic parameters are considered and thus that work deals with two unknowns. However, the approach can be specialized to our context.

⁵ For one of the three equations, the term u_0^4 vanishes, and for a second equation, v_0^4 vanishes. However, this does not influence further conclusions.

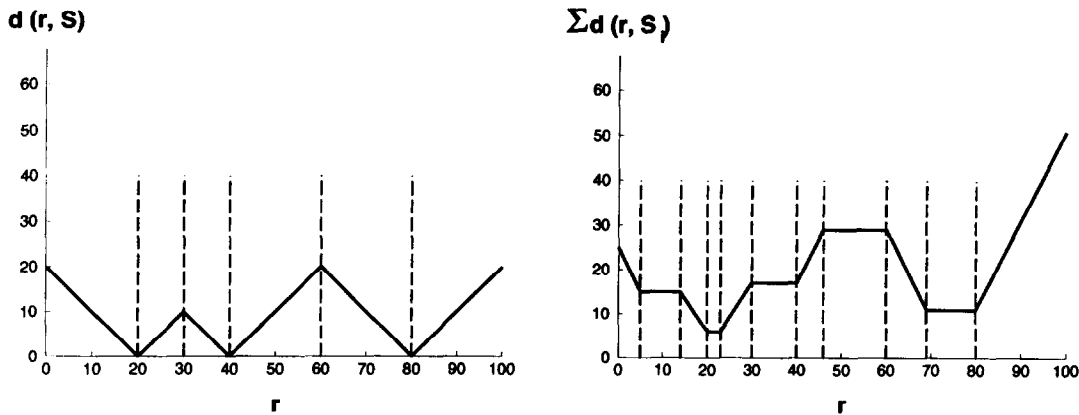


Fig. 3. (a) $d(r, S)$ for $S = \{20, 40, 80\}$. (b) $d(r, S_1) + d(r, S_2)$ for $S_1 = \{20, 40, 80\}$ and $S_2 = \{5, 23, 69\}$. The dotted lines indicate the abscissae where the functions have to be evaluated to find the global minimum.

parameters is given by pre-calibration (see previous section).

For each pair of views, there are three Kruppa equations (only two independent). Let k_{pi} be the i -th Kruppa equation of the p -th pair of views. These equations are polynomials in the sole parameter α_v (see Section 4.2). Thus, α_v is the root which is common to all considered Kruppa equations. To estimate α_v we first compute the roots for each Kruppa equation separately. Since the α_v must be real and positive, only the roots with these properties are retained.

Let

$$S_{pi} = \{r_{pij} \mid j = 1, \dots, n_{pi}\}$$

be the set of real positive roots of the Kruppa equation k_{pi} . We search now for the best approximation of the root which is common to all considered Kruppa equations. In this context we define the “distance” of a number r to a set of numbers $S = \{r_1, \dots, r_n\}$ as

$$d(r, S) = \min_{j=1, \dots, n} |r - r_j|.$$

Hence, the problem can be formulated as finding the real

number r which minimizes

$$\sum_{p,i} d(r, S_{pi}) = \sum_{p,i} \min_{j=1, \dots, n_{pi}} |r - r_{pij}|.$$

We propose a simple practical solution to this problem. Consider Fig. 3a which shows the graph of $d(r, S)$ for a given set $S = \{r_1, \dots, r_n\}$.

The function is piecewise linear and changes its shape only at the abscissae r_j and $\frac{1}{2}(r_j + r_{j+1})$. Thus, to find the global minimum of the sum $\sum_{p,i} d(r, S_{pi})$, it is sufficient to evaluate it at all abscissae r_{pij} and $\frac{1}{2}(r_{pij} + r_{pi,j+1})$ and to pick out the abscissa r for which we get the minimum value. This abscissa is not uniquely defined if we have an even number of Kruppa equations (cf. Fig. 3b, where the global minimum lies between the abscissae 20 and 23). In this case, we choose the middle value.

An example of the graphs of the three Kruppa equations which arise from two views is shown in Fig. 4.

When many views are used for self-calibration, robust methods [12] should be applied for the estimation of the common root.

5.1. Outline of dynamic self-calibration

Step 0. Pre-calibrate the camera, i.e. determine the functional relationship of intrinsic parameters in dependence of α_v (see Section 4.1).

Step 1. Compute the fundamental matrices for pairs of views from correspondences of image points.

Step 2. Compute the coefficients of the powers of α_v in the Kruppa equations (see Section 4.2).

Step 3. Compute the roots of each Kruppa equation and retain the real positive ones (see eqn (5)).

Step 4. α_v is the “best” common root of the Kruppa equations (see eqn (5)).

Step 5. Compute the other intrinsic parameters from α_v , following the functional relationships established in Step 0.

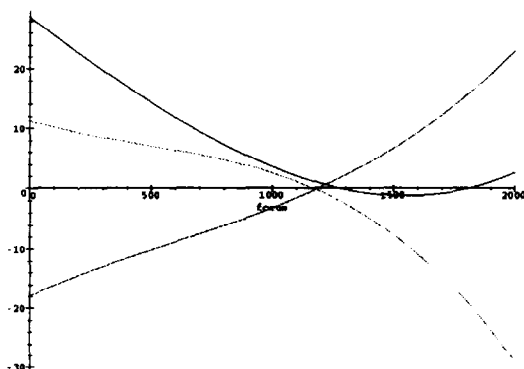


Fig. 4. Example for the graphs of the three Kruppa equations for two views.

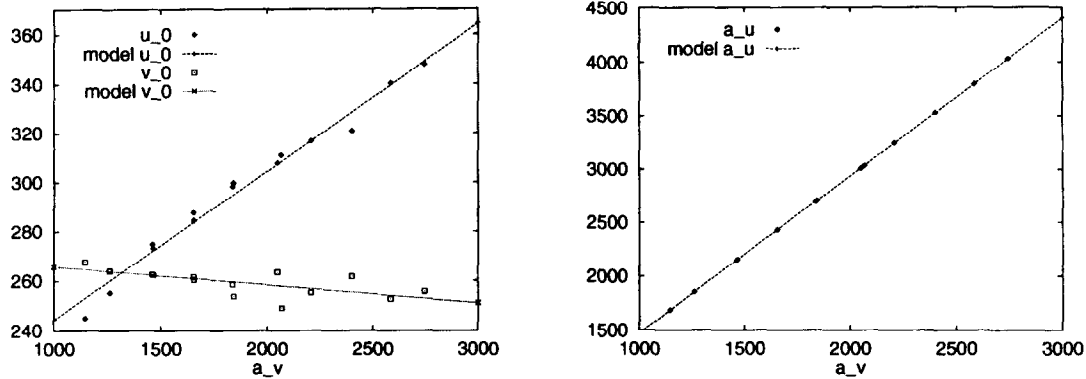


Fig. 5. (a) Coordinates of the principal point (u_0, v_0) with respect to α_v . (b) α_u with respect to α_v . The points in these graphs were obtained by classical calibration using a calibration grid [11]. For each zoom position, several positions of the grid were used. The plotted lines represent the models found for the parameters' interdependence.

6. Experimental evaluation

We have carried out experiments with an E.I.A. Servo-lens zoom, mounted on a Pulnix TM-6EX camera. In a first step, the camera was pre-calibrated. For this purpose, a full off-line calibration was done for various zoom positions, by pointing the camera at a calibration grid. The field of computed intrinsic parameters is shown in Fig. 5, where u_0 , v_0 and α_u are displayed in relation to α_v .

Next, the functional relationship between the intrinsic parameters was modelled. We found the following linear relations:

$$\begin{aligned}\alpha_u &= 1.466\alpha_v, & u_0 &= 0.060\alpha_v + 184.44. \\ v_0 &= -0.007\alpha_v + 273.19.\end{aligned}$$

The skew angle θ is fixed to 90° .

Dynamic self-calibration was then performed by pointing the pre-calibrated camera at the calibration grid, from different viewpoints. We compared our method with an algorithm performing a Levenberg–Marquardt (LM) minimization of the criterion (4). In contrast to our algorithm, this non-linear optimization needs an initialization of the intrinsic parameters. We applied the algorithm on 9 different initializations, which all verified exactly the model

established in pre-calibration and which covered the complete range of considered zoom positions. Furthermore, the LM-algorithm was run in 4 different modes, keeping constant:

- the initial values of the aspect ratio τ and u_0 and v_0 ;
- the initial value of the aspect ratio τ ;
- the initial values of u_0 and v_0 ;
- none of the parameters.

To summarize, one experiment consisted in applying our algorithm without initialization and running the 4 versions of the LM-method, each one with 9 different initializations. 27 different experiments were carried out: for each of 9 zoom positions, 4 images of a calibration grid were taken, and self-calibration was carried out for 2, 3 and all of the images. The estimation of the intrinsic parameters was then evaluated based on a model-based calibration performed with the same images of the calibration grid. In Fig. 6 we summarize the results of the estimation of α_u . Each bar represents the number of experiments for which the relative error of the estimated α_u lies in the corresponding error interval. The upper bars correspond to the method proposed in this paper and the lower ones to the LM-algorithm for which τ , u_0 and v_0 were kept fixed, which has been found to be the best among the different modes.

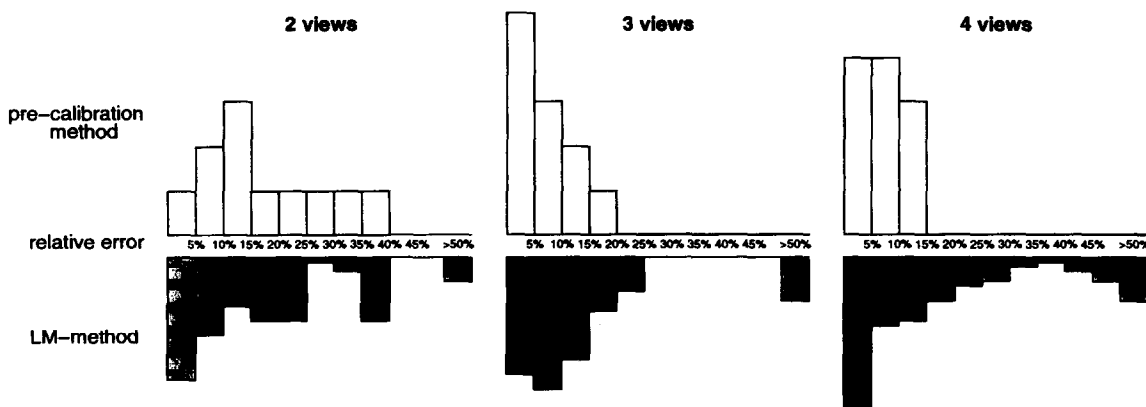


Fig. 6. Results of dynamic self-calibration.

The major conclusion is that, for more than 2 views, our method was not subject to serious failure, contrary to the LM-method, which completely failed in more than 5% of the experiments. However, when the initialization was close to the true values, the LM-method gave also mostly acceptable results.

The graphs for estimation of u_0 and v_0 (not shown here) underline the higher reliability of self-calibration using all available pre-calibration information.

7. Conclusions and further work

We have examined the interdependence of intrinsic parameters of a zooming camera in order to reduce the number of unknowns in self-calibration processes. Especially we have shown that, when the pinhole model is assumed, self-calibration consists in the estimation of only one intrinsic parameter. We propose a special algorithm which exploits the interdependence of the parameters and which is based on an off-line pre-calibration of the camera. The algorithm needs only simple computations (roots of univariate polynomials) and furthermore, no initialization of the parameters is necessary. Experiments have shown, that the proposed method is more reliable than classical non-linear optimization which does not exploit completely the interdependence of the intrinsic parameters.

The major drawback is of course the need of a time-consuming pre-calibration process. It is also not clear if the proposed mechanism will be very effective for imaging systems where the interdependence of parameters follows a more complicated model than the one found with our equipment.

In this paper we have neglected the effect of focusing. This could be dealt with by doing pre-calibration for different focus settings and establishing different interdependence models which then cover the whole range of focus and zoom settings. The method could then be run for these different models and the self-calibration which gives the lowest re-projection residue for the reconstruction of the observed scene, would be retained. This scheme must still be validated experimentally.

The actual implementation of the algorithm could be extended in several directions: the search for the common

root of many Kruppa equations can be done by a robust method. Uncertainty estimates for the fundamental matrices can be taken into account when many views are given. On the experimental side, experiments with more than 4 images and with real images (not a calibration grid) should be undertaken.

Acknowledgements

This work was partially supported by INRIA France. We thank Reg Willson for the kind permission to publish Fig. 1, Philippe Bobet for helpful discussions and Pascal Brand for his help for carrying out the experiments.

References

- [1] S.J. Maybank, O.D. Faugeras, A theory of self calibration of a moving camera, *International Journal of Computer Vision* 8 (2) (1992) 123–151.
- [2] Q.-T. Luong, Matrice fondamentale et autocalibration en vision par ordinateur, Thèse de doctorat, Université de Paris-Sud, Orsay, France, December 1992.
- [3] R. Hartley, Extraction of focal lengths from the fundamental matrix, G.E. CRD, Schenectady, NY, 1993.
- [4] R. Enciso, T. Viéville, Experimentally self-calibration from four views, in: *Proc. 1995 Int. Conf. on Image Analysis and Processing*, San Remo, Italy, September 1995.
- [5] R.G. Willson, S.A. Shafer, A perspective projection camera model for zoom lenses, in: *Proc. 2nd Conf. on Optical 3-D Measurement Techniques*, Zürich, Switzerland, October 1993.
- [6] A.W. Burner, Zoom lens calibration for wind tunnel measurements, in: *Proc. SPIE Conf. on Videometrics IV*, Philadelphia, PA, October 1995, pp. 19–33.
- [7] J.G. Semple, G.T. Kneebone, *Algebraic Projective Geometry*, Oxford Science Publication, Oxford, 1952.
- [8] R.I. Hartley, Euclidean reconstruction from uncalibrated views, in: *Proc. DARPA-ESPRIT Workshop on Applications of Invariants in Computer Vision*, Azores, Portugal, October 1993, pp. 187–202.
- [9] D.C. Brown, Close-range camera calibration, *Photogrammetric Engineering* 37 (8) (1971) 855–866.
- [10] O. Faugeras, What can be seen in three dimensions with an uncalibrated stereo rig?, in: *Proc. 2nd ECCV*, Santa Margherita, Italy, May 1992, pp. 563–578.
- [11] O.D. Faugeras, G. Toscani, Camera calibration for 3D computer vision, in: *Proc. Int. Workshop Machine Vision and Machine Intelligence*, Tokyo, 1987.
- [12] P. Meer, D. Mintz, A. Rosenfeld, D.Y. Kim, Robust regression methods for computer vision: a review, *International Journal of Computer Vision* 6 (1) (1991) 59–70.